



Regular Article

## Red carbon dots-based phosphors for white light-emitting diodes with color rendering index of 92

Yuechen Zhai <sup>a,b</sup>, Yi Wang <sup>c</sup>, Di Li <sup>a</sup>, Ding Zhou <sup>a,\*</sup>, Pengtao Jing <sup>a</sup>, Dezhen Shen <sup>a</sup>, Songnan Qu <sup>a,\*</sup>

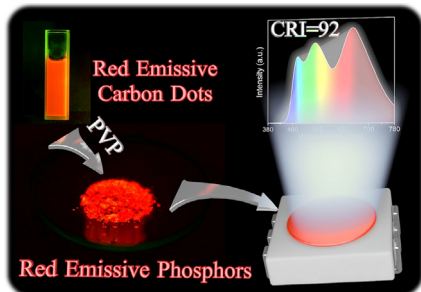
<sup>a</sup> State Key Laboratory of Luminescence and Applications, Changchun Institute of Optics, Fine Mechanics and Physics, Chinese Academy of Sciences, Changchun 130033, PR China

<sup>b</sup> University of Chinese Academy of Sciences, Beijing 100049, PR China

<sup>c</sup> College of Physics, Jilin University, Changchun 130012, PR China



### GRAPHICAL ABSTRACT



### ARTICLE INFO

#### Article history:

Received 6 March 2018

Revised 7 May 2018

Accepted 28 May 2018

Available online 29 May 2018

#### Keywords:

Carbon dots

Red emission

Phosphors

White light-emitting diodes

High color rendering index

### ABSTRACT

Exploration of solid-state efficient red emissive carbon dots (CDs) phosphors is strongly desired for the development of high performance CDs-based white light-emitting diodes (WLEDs). In this work, enhanced red emissive CDs-based phosphors with photoluminescence quantum yields (PLQYs) of 25% were prepared by embedding red emissive CDs (PLQYs of 23%) into polyvinyl pyrrolidone (PVP). Because of the protection of PVP, the phosphors could preserve strong luminescence under long-term UV excitation or being mixed with conventional packaging materials. By applying the red emissive phosphors as the color conversion layer, WLEDs with high color rendering index of 92 and color coordinate of (0.33, 0.33) are fabricated.

© 2018 Elsevier Inc. All rights reserved.

### 1. Introduction

White light-emitting diodes (WLEDs) indicate a promising future in replacing the traditional lighting sources, since they are long-lived, eco-friendly and energy-saving [1–4]. Currently, the most common path of manufacturing the WLEDs is based on phosphors and the blue light-emitting InGaN chip [5]. The phosphors are used as color conversion layer to convert the blue emission

of the InGaN chip into other emission color, and then the residual non-absorbed blue light and emission from phosphors mix to form white light [6]. Thereby, phosphors, as a significant part of WLEDs, play a pivotal role in determining the performance of WLEDs, such as color rendering index (CRI), correlated color temperature (CCT), Commission Internationale de l'Eclairage (CIE) chromaticity coordinate, luminous efficiency, and so forth [7–9]. At present, commercial phosphors are based on the nonrenewable rare-earth materials, while the exploitation of them would often cause the concerns of environmental destruction [10]. Semiconductor quantum dots (QDs) were proposed to be potential alternative as color

\* Corresponding authors.

E-mail addresses: [zhouding@ciomp.ac.cn](mailto:zhouding@ciomp.ac.cn) (D. Zhou), [qusn@ciomp.ac.cn](mailto:qusn@ciomp.ac.cn) (S. Qu).

conversion layer for fabricating WLEDs in the past decade, but the high-performance QDs are often composed of heavy metal elements, such as Cd and Pb, leading to toxicity concerns [11–13]. Perovskite QDs, as an emerging luminescent material, are also expected to be applied for WLEDs. However, their photoluminescent (PL) property could be seriously quenched due to the anion-exchange reaction when being exposed in the air, which restricts their applications as phosphors [14]. Therefore, exploring alternative luminescent materials is an important research avenue to promote the development of LEDs [15,16].

Carbon dots (CDs), an emerging class of carbon-based luminescent nanomaterials, have drawn more and more attention in recent years owing to their outstanding properties, such as chemical stability [17–19], biocompatibility [20–22], photostability [23–26], low toxicity [27–30] and so forth. Because of those distinct merits, CDs could be applied in extensive fields, such as drug delivery, solar cell, optoelectronic devices, bioimaging, and so on [31–44]. Besides, CDs have shown potential to be as a color conversion layer for WLEDs due to their strong luminescence [45]. However, efficient CDs-based phosphors are difficult to achieve, which could be understood in terms of the aggregation-induced luminescence quenching of CDs in the aggregated state [46]. To overcome this problem, several suitable matrices are utilized to ensure the monodispersity of CDs in the solid state, resulting in highly luminescent solid-state materials. For instance, Rogach et al. embedded CDs into polymethylmethacrylate to form luminescent phosphors, and combined the phosphors with ultraviolet (UV) chips to fabricate LEDs [37]. Similarly, in our previous work, CDs were dispersed on the surface of starch, ensuring the monodispersity of CDs and therewith the strong PL emission, which could be used as the color conversion layer for cool WLEDs with CCT of 9892 K [45]. Despite the successes in fabricating LEDs, these approaches still own several limitations for realizing practical illumination. Ideal WLEDs-based illumination source should be based on blue-emitting InGaN chips instead of ultraviolet light to avoid the harm of UV light to the human health [9]. Meanwhile, owing to the lack of efficient red emissive CDs-based phosphors, current CDs-based WLEDs possess low CRI and high CCT, which is not favorable to present the true apparent color [47]. Consequently, it is of great scientific interest and value to develop more efficient routes to prepare CDs-based phosphors for high performance WLEDs with high CRI.

In this work, we prepared red emissive CDs-based phosphors through embedding red emissive CDs (r-CDs) into polyvinyl pyrrolidone (PVP). The as-prepared r-CDs@PVP phosphors exhibit

a red emission located at 648 nm and high photoluminescence quantum yields (PLQYs) of 25% under 532 nm excitation, which could be ascribed to the plentiful electron-acceptor group (C=O) of PVP. Additionally, green emissive phosphors based on green emissive CDs (g-CDs) were synthesized [45], which possess strong PL emission centered at 532 nm with PLQYs of 36% under 450 nm light. These CDs-based phosphors exhibit good photostability and structural stability. Based on these advantages, these two phosphors were deposited successively on the InGaN chip of LEDs in order of decreasing PL emission wavelength. In the WLEDs prototype, blue emission (450 nm) of InGaN chip first excite the g-CDs@starch phosphors to emit green light (532 nm), and then r-CDs@PVP phosphors are excited to generate red light, leading to a broad spectrum emission and thereby achieving WLEDs with high CRI of 92 (Fig. 1).

## 2. Results and discussion

Experimentally, g-CDs are prepared from citric acid and urea by the microwave-assisted heating method [45]. Under sunlight, the diluted solution of g-CDs presents primrose yellow, indicating a strong absorbance of blue light, which is further confirmed by UV-vis absorption spectrum (Fig. S1a). Under 450 nm excitation, g-CDs solution shows strong green emission located at 532 nm (Fig. S1a and b). As shown in Fig. S1c, high resolution transmission electron microscopy (HRTEM) shows that the lattice spacing of g-CDs is 0.21 nm, consistent with the (1 0 0) lattice planes of graphite [32].

To obtain r-CDs, the reaction between citric acid and urea is performed in the solvothermal method as described in MATERIALS AND METHODS. The as-prepared r-CDs are dissolved in dimethylsulfoxide (DMSO), which possesses an obvious absorption in the range of green light (Fig. 2a). Meaningfully, r-CDs presents strong red emission under green light (532 nm) excitation (Fig. 2b), where the electron-acceptor group (S=O) of DMSO is capable of modifying the surface of the r-CDs, thereby influencing the optical bandgap and promoting electron transitions [48]. Furthermore, PLQYs of r-CDs DMSO solution is measured to be 23% under 532 nm excitation. TEM and HRTEM images present monodisperse r-CDs with an average diameter of 3.4 nm and lattice spacing of 0.21 nm, consisting with the (1 0 0) crystallographic facet of graphite (Figs. 2c and S2) [49–52].

To obtain solid-state luminescent materials, these CDs should be dispersed onto matrix to avoid the aggregation-induced

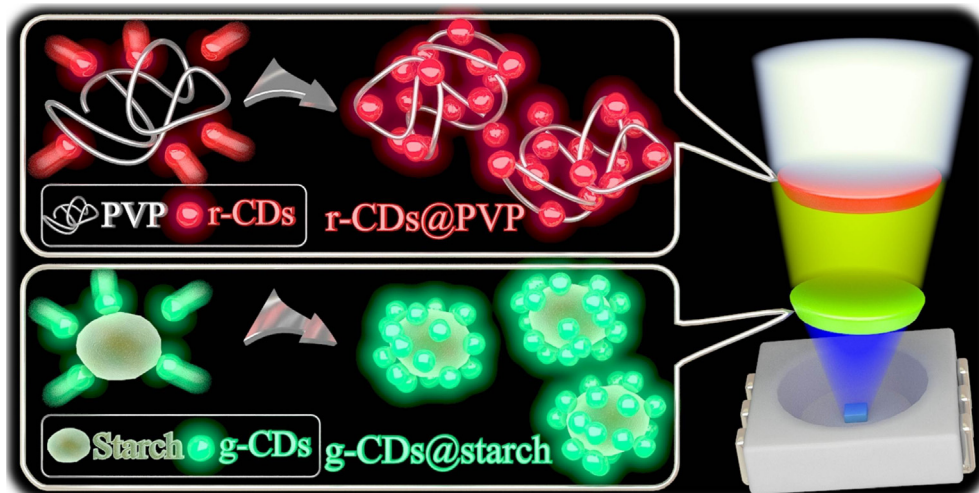


**Fig. 1.** Schematics of preparation of CDs-based phosphors for WLEDs.

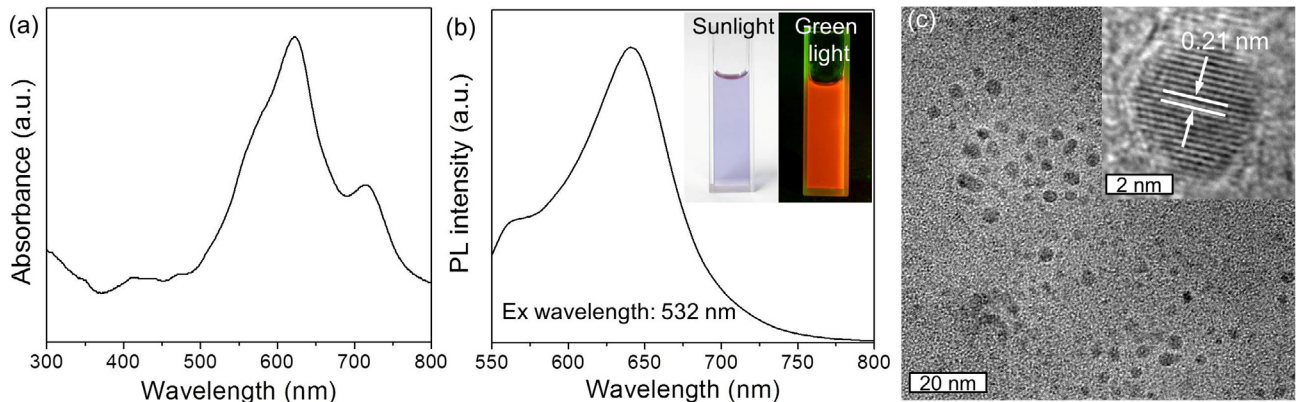


**Fig. 2.** (a) Absorption spectrum of r-CDs DMSO solution. (b) PL emission spectrum of r-CDs DMSO solution under green light (532 nm). Insets in (b) are optical image of r-CDs DMSO solution under sunlight, and the corresponding fluorescent image under green light (532 nm) with a 550 nm filter (long pass). (c) TEM and HRTEM images of r-CDs.

luminescence quenching of CDs. Here, g-CDs solutions are mixed with starches. Since there are lots of hydroxyl groups in g-CDs and starch [45], g-CDs have a strong interaction with the starch through hydrogen bond, resulting in the monodisperse g-CDs on the surface of the starch. Under blue light, the g-CDs@starch phosphors with mass ratio of 1:30 wt% exhibit bright green fluorescence from the g-CDs (Fig. 3a and b), whereas bare starch has no PL emission (Fig. S3). PL emission spectrum of the g-CDs@starch phosphors is nearly identical with that of g-CDs solution, indicating no aggregation of g-CDs on the surface of starch (Figs. 3c and S1). To further confirm this proposal, another two g-CDs@starch phosphors with different mass ratios (1:50 and 1:70 wt%) are prepared (Fig. S4a–d), whose PL emission spectra are same as that of the g-CDs@starch phosphors (mass ratio of 1:30 wt%) (Figs. 3c and S4e), demonstrating the good monodispersity of g-CDs. Similarly, r-CDs are combined with PVP to maintain their stabilization and strong luminescence in the solid state (Fig. 3d and e). The r-CDs@PVP phosphors present red emission under green light (Fig. 3e). The PL emission of the r-CDs@PVP phosphors centers at 650 nm with PLQYs of 25% under 532 nm excitation (Fig. 3f). Compared to the r-CDs DMSO solutions, there is a red-shift in the PL

emission of the r-CDs@PVP phosphors, which is attributed to the variations of the electron-acceptor group from S=O of DMSO to C=O of PVP [48]. But, the longer-wavelength emission is more favorable to enhance CRI of WLEDs.

To further characterize g-CDs@starch and r-CDs@PVP phosphors, fluorescence microscope images of them are obtained. As seen in Fig. 4a and b, under blue and green light, homogeneous green and red emission from the whole phosphors are observed, respectively, suggesting a good distribution of CDs in these matrixes. Moreover, the luminescence lifetimes of r-CDs DMSO solution and r-CDs@PVP phosphors are measured to be 5.1 and 5.2 ns, respectively (Fig. 4c and d), which are nearly identical. The aggregations of CDs usually cause energy loss, which would lead to the decrease of the luminescence lifetime. Thereby, the nearly unchanged luminescence lifetime indicates non-aggregation of r-CDs in r-CDs@PVP phosphors [50,53–55].

Since CDs themselves hold good photostability against UV light, the as-prepared phosphors are expected to possess good photostability, ensuring their PL stability upon irradiation by the chips of LEDs. The photostability is investigated by comparing the PL intensity of the phosphors, including g-CDs@starch, r-CDs@PVP

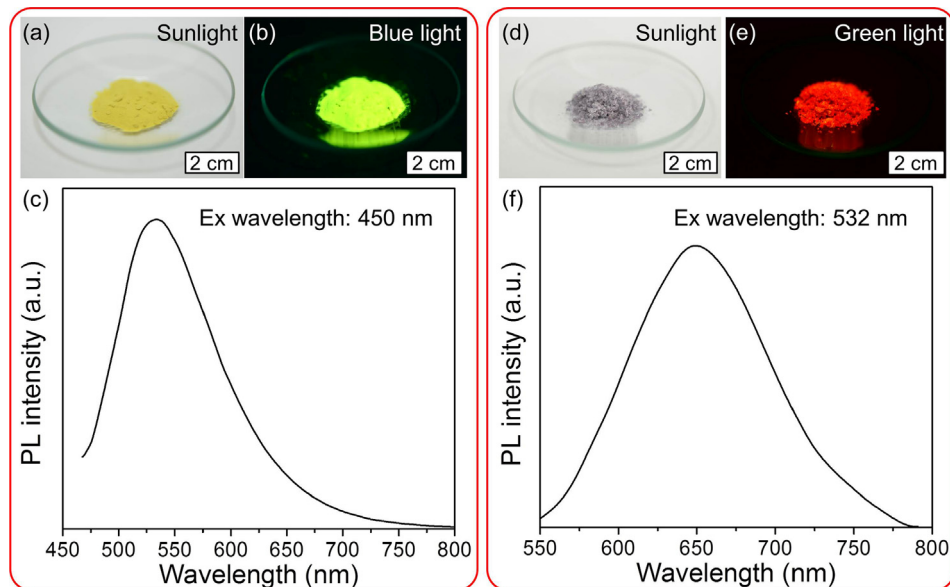


**Fig. 3.** (a) Optical image of g-CDs@starch phosphors with mass ratio of 1:30 under sunlight, and (b) the corresponding fluorescent image under blue light with a 495 nm filter (long pass). (c) PL emission spectrum of g-CDs@starch phosphors under blue light (450 nm). (d) Optical image of r-CDs@PVP phosphors under sunlight, and (e) the corresponding fluorescent image under green light with a 550 nm filter (long pass). (f) PL emission spectrum of r-CDs@PVP phosphors under green light (532 nm).

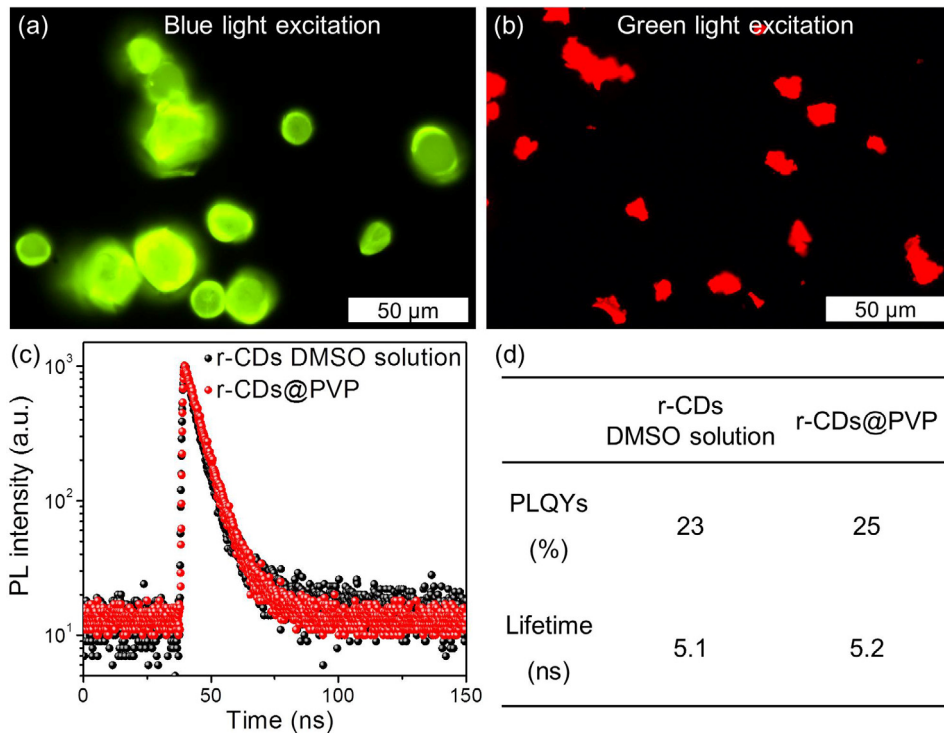


**Fig. 4.** Fluorescence microscope images of (a) g-CDs@starch phosphors and (b) r-CDs@PVP phosphors under blue light and green light, respectively. The exposure time is 100 ms. (c) Luminescence lifetime decay curves of r-CDs DMSO solution (red sphere) and r-CDs@PVP phosphors (black sphere). (d) Comparison of the PLQYs and lifetime of r-CDs DMSO solution and r-CDs@PVP phosphors. (For interpretation of the references to colour in this figure legend, the reader is referred to the web version of this article.)

phosphors and commercial fluorescein sodium (a common fluorescent dye), which are continuously irradiated by a UV light ( $1.6 \text{ W cm}^{-2}$ ) under the same conditions. As seen from Fig. 5a, the harsh conditions of the irradiation used in our tests are indeed harmful to all of the samples. For commercial fluorescent dye, the PL intensity decreases to 80% at first 5 min. After 20 min of irradiation, the PL intensity losses more than a half of its initial PL intensity. After 60 min of irradiation, its PL intensity further decreases to less than 20%. Nevertheless, the PL intensity of g-CDs@starch phosphors decays at a slow rate. Within first 5 min, it losses less than 10%.

As a consequence, about 94% PL intensity of g-CDs@starch phosphors could be retained after 60 min. Furthermore, the photostability of g-CDs@starch phosphors under longer UV light irradiation is tested (Fig. S5). After continuously irradiating g-CDs@starch phosphors for 100 h, their PL intensity could be maintained more than 90%. Similarly, r-CDs@PVP phosphors also possess good photostability against UV light. Within first 5 min, the PL intensity of r-CDs@PVP phosphors reduces less than 5%. After 60 min, the PL intensity of r-CDs@PVP phosphors could be maintained more than 96%. Even under UV light irradiation for 100 h,

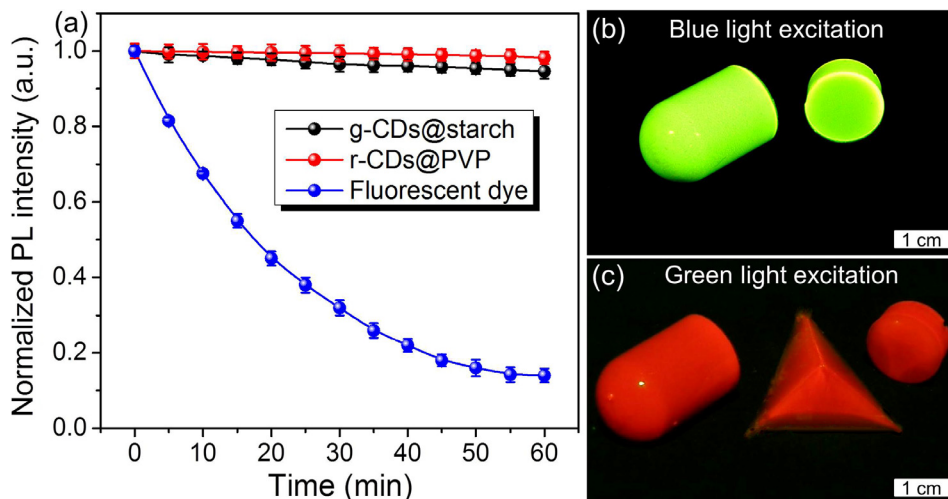


**Fig. 5.** (a) PL intensity decay curves of g-CDs@starch phosphors (black curve), r-CDs@PVP phosphors (red curve) and fluorescent dye (blue curve) under UV light. Images of luminescent bulk materials which are composed of (b) g-CDs@starch phosphors and epoxy-silicone resin under blue light with a 495 nm filter (long pass), and (c) r-CDs@PVP phosphors and epoxy-silicone resin under green light with a 550 nm filter (long pass). (For interpretation of the references to colour in this figure legend, the reader is referred to the web version of this article.)

their PL intensity could still be maintained more than 90% (Fig. S5). Actually, since the intensity of the blue light from the InGaN chips is much weaker than that used in testing the photostability of CDs-based phosphors, the fabricated CDs-based WLEDs is expected to possess much better stability, as evidenced later. Therefore, g-CDs@starch and r-CDs@PVP phosphors possess great potential applications as color conversion layer in LEDs.

Moreover, g-CDs@starch and r-CDs@PVP phosphors could be mixed with commercial packaging materials, such as epoxy-silicone resin, to form various shaped luminescent bulk materials without change of PL emissions in comparison with the initial PL emission of the phosphors (Fig. 5b and c). Under blue light, the materials composed of g-CDs@starch and epoxy-silicone resin can emit bright green light, consisting with the emission of g-CDs@starch phosphors (Fig. 3b). Under green light, the materials composed of r-CDs@PVP and epoxy-silicone resin possess strong red luminescence originating from r-CDs@PVP phosphors (Fig. 3e). These results demonstrate that the PL properties of these phosphors could be well preserved and not deteriorated by epoxy-silicone resin. All above advantages of the CDs-based phosphors allow them to be applied in photoelectric devices.

In fabricating LEDs, the mixtures of the g-CDs@starch phosphors and epoxy-silicone resin are deposited on commercially available blue-emitting InGaN LED chips with an emission peak at 450 nm (Fig. S6), and solidified in an oven at 80 °C for 1 h. When the mass ratio of the g-CDs@starch phosphors and epoxy-silicone resin is 0.6:1 wt%, only cool WLEDs with CIE color coordinate of (0.27, 0.28) and CCT of 12942 K is obtained (Fig. 6a), which is mainly because a small number of phosphors cannot sufficiently convert the blue light from the InGaN chips (the inset of Fig. 6a). Then, the mass ratio of the g-CDs@starch phosphors and epoxy-silicone resin is increased to 2.5:1 wt%, but a yellow green LED

rather than WLED is fabricated, whose CIE color coordinate and CCT are (0.33, 0.40) and 5572 K (Fig. 6b), respectively. The reason why WLEDs cannot be realized is that the g-CDs@starch phosphors can only emit green light and lacks long-wavelength emission (Fig. 3c). Though there is yellow emission in this LEDs, it is mainly due to the reabsorption of g-CDs emission in the phosphors, which has been explained in detail in our previous publication [53]. According to the theory of colorimetry, the CIE color coordinate of the LEDs fabricated by the g-CDs@starch phosphors and InGaN chips can only locate on the line, which is connected by the two CIE color coordinates of the g-CDs@starch phosphors and InGaN chips as shown in Fig. 6c. Meanwhile, owing to the presence of reabsorption, the line should be a curved line (the red line in Fig. 6c). In spite of the incorrect emission color, the LEDs possess low CRI (69) because of lack of red emission (Fig. 6b). To address this issue, the mixtures of r-CDs@PVP phosphors and epoxy-silicone resin are further deposited onto the yellow green LED (Fig. 1). As shown in Fig. 6d, a WLED prototype is produced, showing good color rendition. In the WLEDs, blue emission (450 nm) of InGaN chip first excite the g-CDs@starch phosphors to emit green light (532 nm), and then r-CDs@PVP phosphors are excited to generate red light, leading to a broad spectrum emission and thereby achieving WLEDs with high CRI of 92 (Fig. 6g). To be close to practical applications, an area light composed of nine WLED devices is fabricated (Figs. 6d and S7). Then, some different colored pen caps are used to verify the color rendering property (Fig. 6d). Their apparent colors are almost exactly the same under the WLEDs and sunlight (Fig. 6d and f), demonstrating the high color rendering property of the WLEDs. The luminous efficacy of WLEDs is 12 lm/W at the coordinate of (0.33, 0.33) and CCT of 5610 K (Fig. 6d and e). In addition, due to the good photostability of the g-CDs@starch and r-CDs@PVP phosphors (Fig. S5), the fabricated CDs-based WLEDs

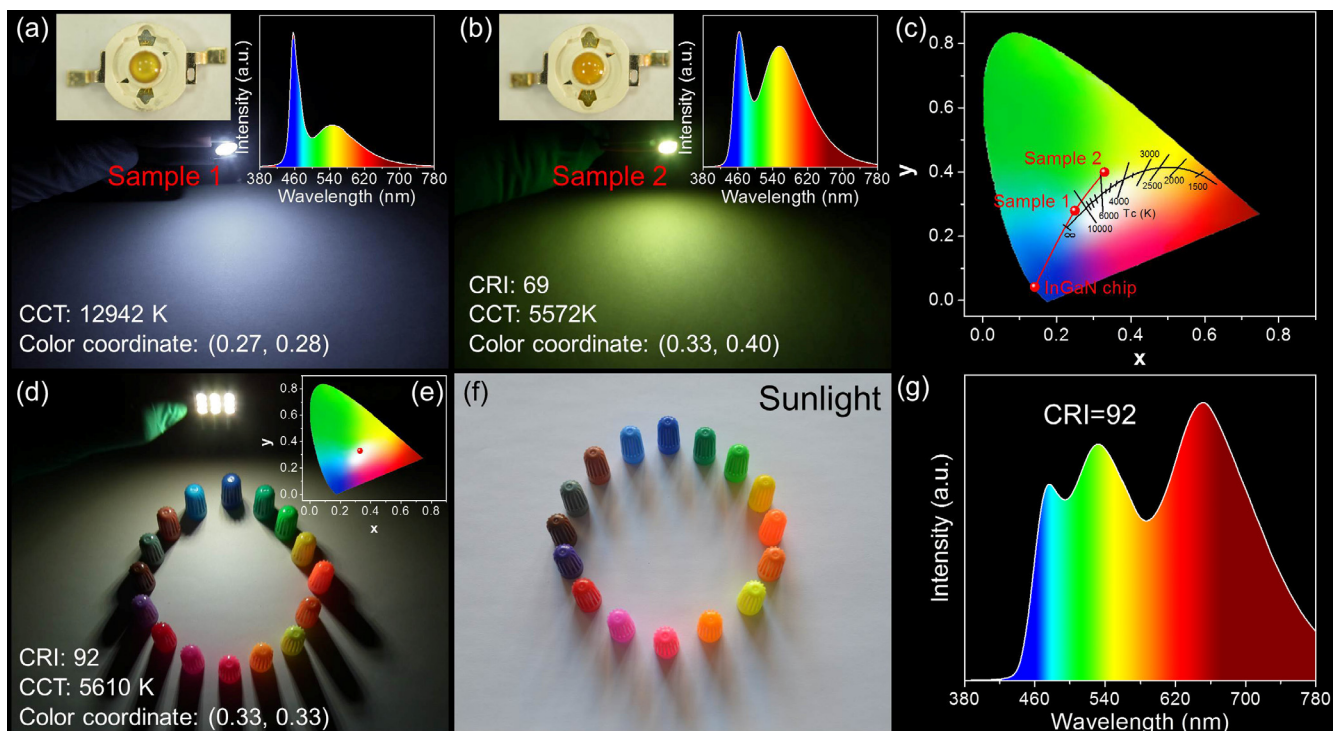


**Fig. 6.** (a) Image of working cool WLED with CIE color coordinate of (0.27, 0.28) and CCT of 12942 K. Insets in (a) are optical image of WLED and emission spectrum of working cool WLED. (b) Image of working yellow green LED with CIE color coordinate of (0.33, 0.40), CCT of 5572 K, and CRI of 69. Insets in (b) are optical image of yellow green LED and emission spectrum of working yellow green LED. (c) CIE chromaticity diagram containing color coordinates of cool WLED and yellow green LED. (d) Image of pen caps with different colors under working WLEDs with CIE color coordinate of (0.33, 0.33), CCT of 5610 K and CRI of 92. (e) CIE chromaticity diagram containing color coordinate of WLEDs with high CRI. (f) Image of pen caps under sunlight. (g) Emission spectrum of working WLEDs as shown in (d). (For interpretation of the references to colour in this figure legend, the reader is referred to the web version of this article.)

possess good stability (Fig. S8). After continuously working for three weeks, the emission intensity of the WLEDs is nearly unchanged. Finally, the WLED is tested at different operation voltage. The decreased voltage only lowers the brightness, but not alters the emission color and CRI (Fig. S9). All these results strongly demonstrate the great potential of the CDs-based phosphors in high performance WLEDs-based illumination applications.

### 3. Conclusions

On the basis of the previous researches, this work has indicated that WLEDs with high color rendition can be realized from r-CDs [33,37,45,53]. The role of PVP in the preparation process of r-CDs@PVP phosphors inhibited the aggregation of r-CDs in the solid state, thus overcoming the aggregation-induced solid-state luminescence quenching. Furthermore, the carbonyl group of PVP as the electron-acceptor group is capable of modifying the surface of the r-CDs, thereby obtaining red emissive phosphors with PL peak position at 650 nm and PLQYs of 25% under 532 nm excitation [48]. Since the protection of PVP and good photostability of CDs themselves, the as-prepared r-CDs@PVP phosphors exhibited good photostability, ensuring their PL stability upon irradiation by the chips of LEDs. After continuously irradiating CDs-based phosphors for 100 h, more than 90% of the emission intensities of CDs-based phosphors could be maintained, indicating the great potential of CDs-based phosphors for practical application. All advantages above allow the r-CDs@PVP phosphors to be used as color conversion layer for enhancing the color rendition of WLEDs. Compared with the g-CDs@starch phosphors-based WLEDs in our previous report [45], the application of the r-CDs@PVP phosphors in color conversion layer can obviously enhance the CRI of WLEDs from 69 to 92. We propose that this synthetic methodology of CDs-based solid-state luminescent materials also expands the way of CDs for wider applications in many other fields.

## 4. Materials and methods

### 4.1. Materials

Starch (98%), urea (99%), citric acid (99.5%) and polyvinyl pyrrolidone (PVP, average mol. Wt. 10,000) were purchased from Gufu, Macklin, and Aladdin, respectively. N,N-dimethylformamide (DMF, 99.5%), dimethyl sulfoxide (DMSO, 99.5%), and ethanol (99.7%) were purchased from Tianjin Fuyu Fine Chemical Co., Ltd.. Sodium hydroxide (NaOH, 96%) and hydrochloric acid (HCl, 36%) were purchased from Tianjin Guangfu Technology Development Co., Ltd. and Beijing Chemical Works, respectively. Epoxy-silicone resin A and B (98%), which were obtained from Ausbond, were used for encapsulation. All of them were not purified before being used.

### 4.2. Synthesis of green emissive CDs (g-CDs)

According to our previous work [45], g-CDs were synthesized in the microwave-assisted heating method. 3 g citric acid and 6 g urea were added into 20 ml deionized water to form transparent solution. Then the pre-blended solution was heated in a domestic 650 W microwave oven for 5 min, during which the solution changed from a colorless clear liquid to a brown and finally a nut-brown solid in aggregated state, indicating the formation of g-CDs. After that, the solid was re-dissolved in deionized water, and centrifuged twice at speed of 8000 rpm for 5 min to remove the aggregated particles. Finally, the solution with green emission under 450 nm light was obtained.

### 4.3. Synthesis of red emissive CDs (r-CDs)

In experiment, r-CDs were synthesized in a solvothermal method. 3 g citric acid and 6 g urea were added into 30 ml DMF and reacted at 160 °C for 6 h under solvothermal condition. Dark-brown solution was obtained after the mixture cooled down to room temperature. Then, the solution was mixed with 3 ml of 50 mg mL<sup>-1</sup> NaOH aqueous solution and 10 ml ethanol, and purified in a centrifuge at the speed of 8000 rpm for 10 min. The precipitates were obtained. After that, the precipitate was further re-dissolved in 3 ml deionized water, mixed with 1 ml of 5 wt% dilute HCl aqueous solution, and centrifuged at the speed of 12,000 rpm for 10 min. The precipitate was collected and re-dissolved in water. The solution was centrifuged three times to wash off residual HCl and salts, and then freeze-dried in vacuum freeze dryer to obtain dark solid of r-CDs.

### 4.4. Preparation of g-CDs@starch phosphors

The g-CDs@starch phosphors (mass ratio: 1:30, 1:50 and 1:70) were prepared by mixing g-CDs with starch in deionized water and stirring for 30 min. The mixtures were filtered to collect the solid blocks on filter paper and freeze-dried in vacuum freeze dryer. Then, the phosphors were ground into powders in agate mortar and collect to be used for experiments and measurements.

### 4.5. Preparation of r-CDs@PVP phosphors

100 mg r-CDs were re-dissolved in 0.5 ml DMSO, and then PVP was added into the solution. After that, the mixtures were put into vacuum to remove the air. The mixtures were dried in vacuum oven at 60 °C for 30 min. Finally, the r-CDs@PVP phosphors were obtained.

### 4.6. Preparation of CDs-based luminescent bulk materials

The g-CDs@starch phosphors were dispersed in the epoxy-silicone resin A and B components (volume ratio: 2:1) under continuously stirring. Then, the mixtures were put into vacuum oven to remove the air, poured into various shaped molds, and baked at 60 °C for 1 h. Finally, green emissive bulk materials with various shapes were obtained. The red emissive bulk materials were prepared in similar way, except using r-CDs@PVP phosphors instead of g-CDs@starch phosphors.

### 4.7. Fabrication of white light-emitting diodes (WLEDs) from g-CDs@starch and r-CDs@PVP phosphors

The commercial InGaN chips with 450 nm emission were used as the WLEDs base. The color conversion layers were prepared by mixing g-CDs@starch or r-CDs@PVP phosphors with epoxy-silicone resin. Then, the mixture was deposited on the InGaN chip of LEDs. After that, LEDs were finally fabricated by curing them at 80 °C for 1 h.

### 4.8. Characterization

Hitachi F-7000 spectrophotometer was used to collect the PL spectra and Shimadzu UV-3010 PC spectrophotometer was used to record the UV-visible absorption spectra. Hitachi H-800 electron microscope was chosen to test the transmission electron microscopy (TEM). The images of products were taken by single lens reflex camera (Nikon D70). The fluorescence microscopy images of composite phosphors were measured by C2+ confocal microscope system (Nikon confocal instruments). In testing the stability

of the CDs-based phosphors, fluorescent dye and WLEDs, each measurement is taken three times, and the average value is used for ensuring the accuracy, though the three values are very much in agreement. The photoluminescence quantum yields (PLQYs) of the r-CDs DMSO solution and CDs-based phosphors were carried out by the calibrated integrating sphere in FLS920 spectrometer. Before the measurement, the instrument was calibrated by the quinine in 0.5 mol/L H<sub>2</sub>SO<sub>4</sub> aqueous solution, where the final concentration was  $1 \times 10^{-5}$  mol/L to eliminate the concentration quenching. The CIE (Commission Internationale de L'Eclairage 1931) colorimetry system was used to authenticate the color of the LEDs.

## Author contributions

The manuscript was written through contributions of all authors. All authors have given approval to the final version of the manuscript.

## Acknowledgment

This work is supported by the National Natural Science Foundation of China (projects No. 51602304), Jilin Province Science and Technology Research (projects No. 20160520008JH, 20150519003JH, 20140101060JC, 20170101191JC, 20170101042JC), and the Open Project Program of the State Key Laboratory of Supramolecular Structure and Materials in Jilin University (No. sklssm201810).

## Appendix A. Supplementary material

Supplementary data associated with this article can be found, in the online version, at <https://doi.org/10.1016/j.jcis.2018.05.101>.

## References

- [1] N. Grandjean, R. Butté, Solid-state lighting on glass, *Nat. Photonics* 5 (2011) 714–715.
- [2] I. Aharonovich, D. Englund, M. Toth, Solid-state single-photon emitters, *Nat. Photonics* 10 (2016) 631–641.
- [3] X.Y. Huang, Red phosphor converts white LEDs, *Nat. Photonics* 8 (2014) 748–749.
- [4] B.Q. Liu, L. Wang, D.Y. Gao, J.H. Zou, H.L. Ning, J.B. Peng, Y. Cao, Extremely high-efficiency and ultrasimplified hybrid white organic light-emitting diodes exploiting double multifunctional blue emitting layers, *Light: Sci. Appl.* 5 (2016) e16137.
- [5] P.P. Dai, C. Li, X.T. Zhang, J. Xu, X. Chen, X.L. Wang, Y. Jia, X.J. Wang, Y.C. Liu, A single Eu<sup>2+</sup>-activated high-color-rendering oxychloride white-light phosphor for white-light-emitting diodes, *Light: Sci. Appl.* 5 (2016) e16024.
- [6] P. Pust, V. Weiler, C. Hecht, A. Tucks, A.S. Wochnik, A.K. Henns, D. Wiechert, C. Scheu, P.J. Schmidt, W. Schnick, Narrow-band red-emitting Sr[LiAl<sub>3</sub>N<sub>4</sub>]:Eu<sup>2+</sup> as a next-generation LED-phosphor material, *Nat. Mater.* 13 (2014) 891–896.
- [7] X.F. Li, J.D. Budai, F. Liu, J.Y. Howe, J.H. Zhang, X.J. Wang, Z.J. Gu, C.J. Sun, R.S. Meltzer, Z.W. Pan, New yellow Ba<sub>0.93</sub>Eu<sub>0.07</sub>Al<sub>2</sub>O<sub>4</sub> phosphor for warm-white light-emitting diodes through single-emitting-center conversion, *Light: Sci. Appl.* 2 (2013) e50.
- [8] L. Wang, R.J. Xie, Y.Q. Li, X.J. Wang, C.G. Ma, D. Luo, T. Takeda, Y.T. Tsai, R.S. Liu, N. Hirosaki, Ca<sub>1-x</sub>Li<sub>x</sub>Al<sub>1-x</sub>Si<sub>1-x</sub>N<sub>3</sub>:Eu<sup>2+</sup> solid solutions as broadband, color-tunable and thermally robust red phosphors for superior color rendition white light-emitting diodes, *Light: Sci. Appl.* 5 (2016) e16155.
- [9] Q.Q. Dai, C.E. Duty, M.Z. Hu, Semiconductor-nanocrystals-based white light-emitting diodes, *Small* 6 (2010) 1577–1588.
- [10] S.H. Lim, Y.H. Ko, C. Rodriguez, S.H. Gong, Y.H. Cho, Electrically driven, phosphor-free, white light-emitting diodes using gallium nitride-based double concentric truncated pyramid structures, *Light: Sci. Appl.* 5 (2016) e16030.
- [11] S. Abe, J.J. Joos, L.I.D.J. Martin, Z. Hens, P.F. Smet, Hybrid remote quantum dot/powder phosphor designs for display backlights, *Light: Sci. Appl.* 6 (2017) e16271.
- [12] E. Jang, S. Jun, H. Jang, J. Lim, B. Kim, Y. Kim, White-light-emitting diodes with quantum dot color converters for display backlights, *Adv. Mater.* 22 (2010) 3076–3080.
- [13] M. Adam, N. Gaponik, A. Eychmuller, T. Erdem, Z. Soran-Erdem, H.V. Demir, Colloidal nanocrystals embedded in macrocrystals: methods and applications, *J. Phys. Chem. Lett.* 7 (2016) 4117–4123.
- [14] C. Sun, Y. Zhang, C. Ruan, C.Y. Yin, X.Y. Wang, Y.D. Wang, W.W. Yu, Efficient and stable white LEDs with silica-coated inorganic perovskite quantum dots, *Adv. Mater.* 28 (2016) 10088–10094.
- [15] Y.P. Sun, B. Zhou, Y. Lin, W. Wang, K.A. Fernando, P. Pathak, M.J. Meziani, B.A. Harruff, X. Wang, H.F. Wang, P.G. Luo, H. Yang, M.E. Kose, B.L. Chen, L.M. Veca, S.Y. Xie, Quantum-sized carbon dots for bright and colorful photoluminescence, *J. Am. Chem. Soc.* 128 (2006) 7756–7757.
- [16] F. Wang, S.P. Pang, L. Wang, Q. Li, M. Kreiter, C.Y. Liu, One-step synthesis of highly luminescent carbon dots in noncoordinating solvents, *Chem. Mater.* 22 (2010) 4528–4530.
- [17] X.W. Xu, K. Zhang, L. Zhao, C. Li, W.H. Bu, Y.Q. Shen, Z.Y. Gu, B. Chang, C.Y. Zheng, C.T. Lin, H.C. Sun, B. Yang, Aspirin-based carbon dots, a good biocompatibility of material applied for bioimaging and anti-inflammation, *ACS Appl. Mater. Interfaces* 8 (2016) 32706–32716.
- [18] B.B. Campos, C. Abellán, M. Zougagh, J. Jimenez-Jimenez, E. Rodríguez-Castellón, J.C.G. Esteves da Silva, A. Ríos, M. Algarra, Fluorescent chemosensor for pyridine based on N-doped carbon dots, *J. Colloid Interface Sci.* 458 (2015) 209–216.
- [19] K.A. Fernando, S. Sahu, Y. Liu, W.K. Lewis, E.A. Gulantis, A. Jafriyan, P. Wang, C. E. Bunker, Y.P. Sun, Carbon quantum dots and applications in photocatalytic energy conversion, *ACS Appl. Mater. Interfaces* 7 (2015) 8363–8376.
- [20] D. Qu, M. Zheng, J. Li, Z.G. Xie, Z.C. Sun, Tailoring color emissions from N-doped graphene quantum dots for bioimaging applications, *Light: Sci. Appl.* 4 (2015) e364.
- [21] D.W. Zheng, B. Li, C.X. Li, J.X. Fan, Q. Lei, C. Li, Z.S. Xu, X.Z. Zhang, Carbon-dot-decorated carbon nitride nanoparticles for enhanced photodynamic therapy against hypoxic tumor via water splitting, *ACS Nano* 10 (2016) 8715–8722.
- [22] O. Kozák, M. Sudolská, G. Pramanik, P. Cigler, M. Otyepka, R. Zbořil, Photoluminescent carbon nanostructures, *Chem. Mater.* 28 (2016) 4085–4128.
- [23] J. Zhang, L. Yang, Y. Yuan, J. Jiang, S.H. Yu, One-pot gram-scale synthesis of nitrogen and sulfur embedded organic dots with distinctive fluorescence behaviors in free and aggregated states, *Chem. Mater.* 28 (2016) 4367–4374.
- [24] V. Lauth, B. Loretz, C.M. Lehr, M. Maas, K. Rezwan, Self-assembly and shape control of hybrid nanocarriers based on calcium carbonate and carbon nanodots, *Chem. Mater.* 28 (2016) 3796–3803.
- [25] H. Gao, A.V. Sapelkin, M.M. Titirici, G.B. Sukhorukov, *In situ* synthesis of fluorescent carbon dots/polyelectrolyte nanocomposite microcapsules with reduced permeability and ultrasound sensitivity, *ACS Nano* 10 (2016) 9608–9615.
- [26] S. Muthulingam, I.H. Lee, P. Uthirakumar, Highly efficient degradation of dyes by carbon quantum dots/N-doped zinc oxide (CQD/N-ZnO) photocatalyst and its compatibility on three different commercial dyes under daylight, *J. Colloid Interface Sci.* 455 (2015) 101–109.
- [27] Z.B. Zheng, J.T. Li, T. Ma, H.L. Fang, W.C. Ren, J. Chen, J.C. She, Y. Zhang, F. Liu, H. J. Chen, S.Z. Deng, N.S. Xu, Tailoring of electromagnetic field localizations by two-dimensional graphene nanostructures, *Light: Sci. Appl.* 6 (2017) e17057.
- [28] K. Bera, A. Sau, P. Mondal, R. Mukherjee, D. Mookherjee, A. Metya, A.K. Kundu, D. Mandal, B. Satpati, O. Chakrabarti, S. Basu, Metamorphosis of ruthenium-doped carbon dots: In search of the origin of photoluminescence and beyond, *Chem. Mater.* 28 (2016) 7404–7413.
- [29] A.R. Chowdhuri, T. Singh, S.K. Ghosh, S.K. Sahu, Carbon dots embedded magnetic nanoparticles @chitosan @metal organic framework as a nanoprobe for pH sensitive targeted anticancer drug delivery, *ACS Appl. Mater. Interfaces* 8 (2016) 16573–16583.
- [30] J. Jiao, C. Liu, X. Li, J. Liu, D.H. Di, Y. Zhang, Q.F. Zhao, S.L. Wang, Fluorescent carbon dot modified mesoporous silica nanocarriers for redox-responsive controlled drug delivery and bioimaging, *J. Colloid Interface Sci.* 483 (2016) 343–352.
- [31] S. Kalytchuk, K. Polakova, Y. Wang, J.P. Froning, K. Cepe, A.L. Rogach, R. Zboril, Carbon dot nanothermometry: Intracellular photoluminescence lifetime thermal sensing, *ACS Nano* 11 (2017) 1432–1442.
- [32] H. Ding, S.B. Yu, J.S. Wei, H.M. Xiong, Full-color light-emitting carbon dots with a surface-state-controlled luminescence mechanism, *ACS Nano* 10 (2016) 484–491.
- [33] Y.H. Chen, M.T. Zheng, Y. Xiao, H.W. Dong, H.R. Zhang, J.L. Zhuang, H. Hu, B.F. Lei, Y.L. Liu, A self-quenching-resistant carbon-dot powder with tunable solid-state fluorescence and construction of dual-fluorescence morphologies for white light-emission, *Adv. Mater.* 28 (2016) 312–318.
- [34] S.J. Zhu, Y.B. Song, X.H. Zhao, J.R. Shao, J.H. Zhang, B. Yang, The photoluminescence mechanism in carbon dots (graphene quantum dots, carbon nanodots, and polymer dots): current state and future perspective, *Nano Res.* 8 (2015) 355–381.
- [35] X.T. Zheng, A. Ananthanarayanan, K.Q. Luo, P. Chen, Glowing graphene quantum dots and carbon dots: properties, syntheses, and biological applications, *Small* 11 (2015) 1620–1636.
- [36] Y. Wang, S. Kalytchuk, L.Y. Wang, O. Zhovtiuk, K. Cepe, R. Zboril, A.L. Rogach, Carbon dot hybrids with oligomeric silsesquioxane: solid-state luminophores with high photoluminescence quantum yield and applicability in white light emitting devices, *Chem. Commun.* 51 (2015) 2950–2953.
- [37] C. Sun, Y. Zhang, K. Sun, C. Reckmeier, T.Q. Zhang, X.Y. Zhang, J. Zhao, C.F. Wu, W.W. Yu, A.L. Rogach, Combination of carbon dot and polymer dot phosphors for white light-emitting diodes, *Nanoscale* 7 (2015) 12045–12050.
- [38] L.L. Pan, S. Sun, A.D. Zhang, K. Jiang, L. Zhang, C.Q. Dong, Q. Huang, A.G. Wu, H. W. Lin, Truly fluorescent excitation-dependent carbon dots and their applications in multicolor cellular imaging and multidimensional sensing, *Adv. Mater.* 27 (2015) 7782–7787.

- [39] S. Khan, A. Gupta, N.C. Verma, C.K. Nandi, Time-resolved emission reveals ensemble of emissive states as the origin of multicolor fluorescence in carbon dots, *Nano Lett.* 15 (2015) 8300–8305.
- [40] K. Jiang, S. Sun, L. Zhang, Y. Lu, A.G. Wu, C.Z. Cai, H.W. Lin, Red, green, and blue luminescence by carbon dots: full-color emission tuning and multicolor cellular imaging, *Angew. Chem. Int. Ed.* 54 (2015) 5360–5363.
- [41] S.L. Hu, A. Trinchia, P. Atkin, I. Cole, Tunable photoluminescence across the entire visible spectrum from carbon dots excited by white light, *Angew. Chem. Int. Ed.* 54 (2015) 2970–2974.
- [42] L. Bao, C. Liu, Z.L. Zhang, D.W. Pang, Photoluminescence-tunable carbon nanodots: surface-state energy-gap tuning, *Adv. Mater.* 27 (2015) 1663–1667.
- [43] C.Q. Ding, A.W. Zhu, Y. Tian, Functional surface engineering of C-dots for fluorescent biosensing and in vivo bioimaging, *Acc. Chem. Res.* 47 (2014) 20–30.
- [44] J.C. Bian, C. Huang, L.Y. Wang, T. Hung, W.A. Daoud, R.Q. Zhang, Carbon dot loading and TiO<sub>2</sub> nanorod length dependence of photoelectrochemical properties in carbon dot/TiO<sub>2</sub> nanorod array nanocomposites, *ACS Appl. Mater. Interfaces* 6 (2014) 4883–4890.
- [45] M.Y. Sun, S.N. Qu, Z.D. Hao, W.Y. Ji, P.T. Jing, H. Zhang, L.G. Zhang, J.L. Zhao, D.Z. Shen, Towards efficient solid-state photoluminescence based on carbon-nanodots and starch composites, *Nanoscale* 6 (2014) 13076–13081.
- [46] D. Zhou, D. Li, P.T. Jing, Y.C. Zhai, D.Z. Shen, S.N. Qu, A.L. Rogach, Conquering aggregation-induced solid-state luminescence quenching of carbon dots through a carbon dots-triggered silica gelation process, *Chem. Mater.* 29 (2017) 1779–1787.
- [47] S.N. Qu, D. Zhou, D. Li, W.Y. Ji, P.T. Jing, D. Han, L. Liu, H.B. Zeng, D.Z. Shen, Toward efficient orange emissive carbon nanodots through conjugated sp<sup>2</sup>-domain controlling and surface charges engineering, *Adv. Mater.* 28 (2016) 3516–3521.
- [48] D. Li, P.T. Jing, L.H. Sun, Y. An, X.Y. Shan, X.H. Lu, D. Zhou, D. Han, D.Z. Shen, Y.C. Zhai, S.N. Qu, R. Zboril, A.L. Rogach, Near-infrared excitation/emission and multiphoton-induced fluorescence of carbon dots, *Adv. Mater.* 30 (2018) e1705913.
- [49] S.H. Li, L.Y. Wang, C.C. Chusuei, V.M. Suarez, P.L. Blackwelder, M. Micic, J. Orbulescu, R.M. Leblanc, Nontoxic carbon dots potently inhibit human insulin fibrillation, *Chem. Mater.* 27 (2015) 1764–1771.
- [50] C. Liu, L. Bao, B. Tang, J.Y. Zhao, Z.L. Zhang, L.H. Xiong, J. Hu, LL. Wu, D.W. Pang, Fluorescence-converging carbon nanodots-hybridized silica nanosphere, *Small* 12 (2016) 4702–4706.
- [51] S.K. Bhunia, L. Zeiri, J. Manna, S. Nandi, R. Jelinek, Carbon-dot/silver-nanoparticle flexible sers-active films, *ACS Appl. Mater. Interfaces* 8 (2016) 25637–25643.
- [52] L. Wang, H.R. Zhang, X.H. Zhou, Y.L. Liu, B.F. Lei, Preparation, characterization and oxygen sensing properties of luminescent carbon dots assembled mesoporous silica microspheres, *J. Colloid Interface Sci.* 478 (2016) 256–262.
- [53] D. Zhou, Y.C. Zhai, S.N. Qu, D. Li, P.T. Jing, W.Y. Ji, D.Z. Shen, A.L. Rogach, Electrostatic assembly guided synthesis of highly luminescent carbon-nanodots@BaSO<sub>4</sub> hybrid phosphors with improved stability, *Small* 13 (2017) 1602055.
- [54] S.A. Crooker, J.A. Hollingsworth, S. Tretiak, V.I. Klimov, Spectrally resolved dynamics of energy transfer in quantum-dot assemblies: towards engineered energy flows in artificial materials, *Phys. Rev. Lett.* 89 (2002) 186802.
- [55] Z.C. Liang, M.J. Kang, G.F. Payne, X.H. Wang, R.C. Sun, Probing energy and electron transfer mechanisms in fluorescence quenching of biomass carbon quantum dots, *ACS Appl. Mater. Interfaces* 8 (2016) 17478–17488.